Geophysical Prospecting

EAGE EUROPEAN ASSOCIATION OF GEOSCIENTISTS & ENGINEERS

Geophysical Prospecting, 2015 doi: 10.1111/1365-2478.12248

Evidence for a new regional NW–SE fault and crustal structure in Tunisia derived from gravity data

Mohamed Arfaoui[1,3]*, Alan Reid[2,4] and Mohamed Hedi Inoubli[3]

[1]*Office National des Mines, BP no. 215, 1080 Tunis, Tunisia,* [2]*Reid Geophysics Ltd, 7 Keymer House, Michel Grove, Eastbourne, BN21 1JZ, U.K.,* [3]*Unité de Recherche de Géophysique Appliquée aux Matériaux et aux Minerais, Université Tunis-El Manar, Faculté des Sciences de Tunis, 2092 El Mana, Tunis, Tunisia, and* [4]*School of Earth & Environment, University of Leeds, Leeds, LS2 9JT, U.K.*

Received July 2013, revision accepted January 2015

ABSTRACT

A new Tunisian gravity map interpretation based on the Gaussian filtered residual anomaly, total horizontal gradient, and Moho discontinuity morphology established from gravity data exhibit a new regional northwest–southeast fault extending from Eastern Kairouan to Ghardimaou (Algeria–Tunisia Boundary). It presents a horizontal gradient maximum lineament that terminates the north–south Jurassic structures in the Kairouan plain. Further, this interpretation reveals other known fault systems and crustal structures in Tunisia. The new regional northwest–southeast fault constitutes with the north–south axis and Gafsa–Jefara faults the deepest faults coinciding with the Moho flexures, which had an important role in their initiation. They constitute the border intra-continental crust faults of the Mesozoic rift. The newly recognized deep fault has critical implications for mineral and petroleum perspectives.

INTRODUCTION

Crustal strike-slip faults are of considerable structural importance and have an indirect economic implication because they are of significance for recognition of sedimentary structure evolution. Crustal faults play a significant role in the formation of:

- folds and faults, which commonly constitute structural traps to accumulate hydrocarbons;
- economic mineral deposits by controlling the migration of hydrothermal fluids.

The delineation of economic reserves of valuable mineral deposits and hydrocarbon accumulations include generally the study of the relation between basement morphology and sedimentary basins and the relation between shallow and deep faults.

Examination of Tunisian deep structures and their evolution has required a combination of geological studies and large-scale regional geophysical surveys. Thus, Tunisia has been the focus of several regional geophysics investigations since 1940. The first gravimetric campaigns were completed in 1947, and a regional aero-magnetic survey covered all of Tunisia in 1964. The requirement for a gravity map covering the entire country was fulfilled by compiling data from various gravimetric campaigns carried out by oil companies, the results of this work mainly discussed the structure of the lithosphere (Jallouli and Mickus 2000; Mickus and Jallouli 1999). Knowledge of deep structures in Tunisia was enormously enriched by the results of a seismic survey carried out by Geo Traverse in 1985 (Buness *et al.* 1992). Thus, regional geophysical surveys have contributed greatly to the characterization of deep structures in Tunisia. However, some interpretations are affected by poor quality data, and others are still hypothetical or have been based on a single profile model; therefore, they cannot be extended to the entire Tunisian surface.

In spite of the poor data quality in certain profiles and the low sampling density, the airborne magnetic survey results reveal the shape and depth of a magnetic basement situated at a depth of 2 km in the extreme North of Tunisia, which may be in concordance with Archaean granitic basement outcrops in Eastern Algeria. In the Atlas, the magnetic basement appears

*E-mail: m.arfaoui4@voila.fr

with a convexity at a depth of 4 km, which separates two different tectonic zones in the South. The magnetic basement increases to a depth of 4 km in the Eastern Mednine region and south of Chotts, where its structure is interpreted as an anticline with NW–SE axis.

Several authors have discussed the results of the seismic reflection/refraction profile observed by the European Geotraverse Project for lithosphere recognition. Morelli and Nicolich (1990) presented a cross section of the lithosphere along the European Geotraverse southern segment from the Alps to Tunisia, which showed a Moho that deepens from a depth of 20 km on the north coast to 35 km in the extreme north and 40 km in the Atlas. Buness *et al.* (1992) proved in their seismic model of an N–S profile segment of Tunisia that thick sediment reached 14 km in the Tunisian furrow and 12 km in the Gafsa furrow. The authors presented a tentative Moho contour map of the surveyed area of Tunisia, in which the crust thickness was approximately 22 km in the north and 37 km in the Atlas.

Mickus and Jallouli (1999) and Jallouli and Mickus (2000) remodelled the N–S profile based on Tunisian gravimetric data and provided new information about the deep structure that remained associated with the profile, which cannot be generalized elsewhere. In those studies, it was revealed that:

(i) a thickened crust in the South of the Saharan flexure (32–38 km thick) coupled with a reduction of the Paleozoic and Mesozoic sediment thicknesses (2–3 km) and a crust thickening in the Atlas of 35 km that decreases towards the north (26 km) contributing to thick Palaeozoic, Mesozoic, and Cenozoic sediments (12 km);
(ii) a thick Cenozoic filling of the basins in the Tunisian furrow (1–2 km);
(iii) the Triassic is significantly thicker in the north than the south and begins to increase in the north.

A residual anomaly model presented by Jallouli and Mickus (2000) shows sediments and upper crust thickness variations from the north to the south of Tunisia without any indication of the gravity effect from major faults. None of the Tunisia gravity studies discuss the large Bouguer anomaly gradient lineaments.

None of the geophysical studies used for the recognition of Tunisian deep structure indicate the presence of deep faults, although the major fault systems that affect the crust such as the Jeffara–Gafsa, Teboursouk, and N–S faults have been the subject of many geological studies since the work of Glangeaud (1951), Dubourdieu (1956), Castany (1951), Jauzein (1967), Zargouni (1985), Boukadi (1996), Martinez and Truillet (1987) and Bouaziz *et al.* (2002).

In this paper, we use Woollard's (1959) empirical relation between crust thickness and Bouguer anomaly to determine the depth, shape, and flexure of Moho discontinuity over all of Tunisia. Then, horizontal gradient grid peaks of Bouguer anomaly and optimal upward continuation have been performed to determine, respectively, superficial and deep fault systems.

TUNISIAN GEOLOGY SETTING

Sited in North Africa, Tunisia includes geologic outcrops that extend in age from the first era to the recent quaternary. Outcrop diversity results from the juxtaposition of two different African domains sharply separated by the Jefara–Gafsa fault system: the Alpine domain, including the Tell and Atlas zones structured essentially at the Mesozoic and Cenozoic, and the stable Saharan platform that belongs to the old African basement. The nearest Archaean granitic basement outcrop appears in Eastern Algeria, which may be in concordance with the basement of Northern Tunisia.

The tectonic setting of Tunisia is an integral part of North African tectonics recognized mainly by:

(i) The Tethyan extensional event corresponding to Early Mesozoic rifting of the North Africa margin (Snoke, Schamel, and Karasek 1988) and massive subsidence during the Jurassic, Triassic and early Cretaceous. This extension has largely controlled sedimentation by the activation of NE–SW, NW–SE, and N–S deep faults; limited extensional events were recognized equally at Late Cretaceous and Tertiary times (Martinez and Truillet 1987).
(ii) The compressional tectonic event associated with the Alpine orogeny remained active from the late Cretaceous to recent time. It caused the inversion of normal faults, reactivation of uplifts, and intrusion of Triassic evaporate diapirs (Ben Ferjani, Burrolet, and Mejri 1990; Bouaziz *et al.* 2002).

Tectonic movements have controlled sedimentation by the activation of NE–SW, NW–SE, and N–S deep paleo-faults and fashioned structures by erecting anticlines, synclines, and collapsed troughs. Thus, five major structural zones can be distinguished in Tunisia by their historical geology and constituents, known from north to south as: the nappe zone, diapiric zone, Atlas zone, the N–S Axis, eastern platform, and Saharan platform (Fig. 1a). The boundaries of these zones are generally marked by faults.

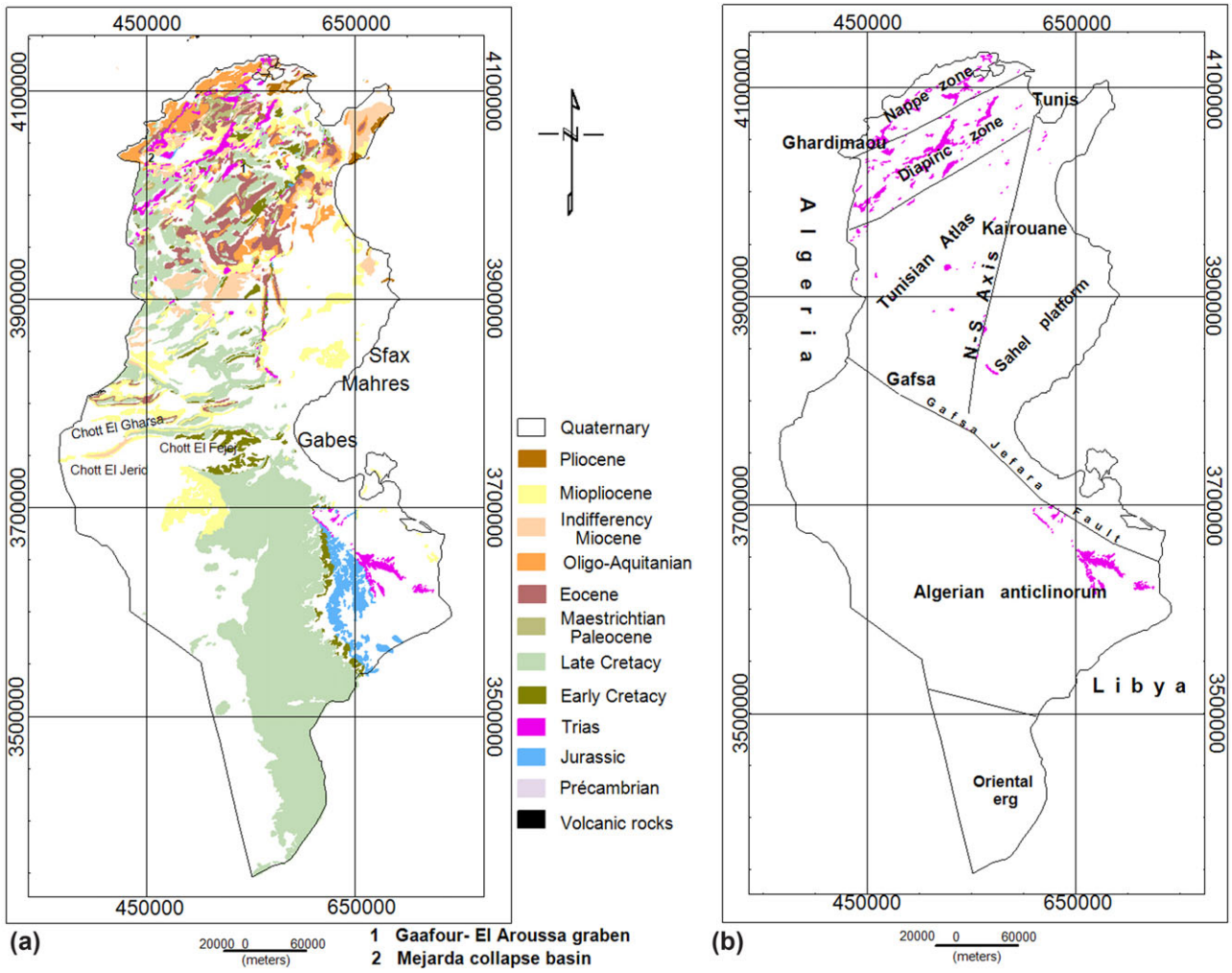

Figure 1 (**a**) Geological map of Tunisia. (**b**) Major structural provinces.

In the extreme north, the nappe zone proposed by Jauzein (1967) and Rouvier (1977) is characterized by allochthonous units formed by Numidian clays and sandstones. Local outcrops of acid volcanic rocks and basalts occur in this zone (Rouvier 1977; Ouazaa 2000).

A diapiric zone formed in the Tunisian furrow during the Mesozoic (Bolze, Burollet, and Castany 1952) and largely deformed during the compressional tectonic event is distinguished by Triassic evaporite outcrops that occupy anticline cores and follow major faults (Perthuisot 1978, 1981).

The Tunisian Atlas comprises thin platform sediments (Burollet 1956), which have been folded into large NE–SW anticlines and synclines. Thereafter, they have been cut by NW–SE border faults of Mio-Plio-Quaternary troughs (Jauzein 1967; Turki 1985).

The N–S axis composed of N–S structures corresponds to a sedimentary limit between two domains, which have different paleogeographic settings, i.e., the Atlas zone and the Eastern platform. This alignment formed a paleogeographic feature since the Jurassic as the reductions or condensations of the sedimentary sequences often show gaps and discordances.

The Eastern platform, extending east of the N–S axis, is characterized by a slow subsidence during the Mesozoic and more active subsidence during the Cenozoic (Burollet and Byramjee 1974). At surface, the eastern platform presents folding tectonics marked by large Mio-Plio-Quaternary folds and appears unaffected by faulting but, in depth, shows a structure of horsts and grabens, which are the result of NE–SW, NW–SE, and N–S fault activities (Fig. 1b) (Haller 1983).

The Saharan platform zone, fringed to the north by the Gafsa fault and the huge endorheic salted basins of El Jerid and

El Fejej Chotts, remained stable during the whole Mesozoic and Cenozoic, and was affected only by epeirogenic movements (Bishop 1975).

A review of the vicinity zones of Tunisian major fault systems reveals important contrasts and gaps in sedimentary series, strike-slip structure, overlapping, flexures, unconformities, and facies changes. In some cases these faults have constituted an important paleogeographic limit. Other faults extend by Triassic salt structures (such as the Teboursouk fault) or associate with volcanism and hydrothermalism. Following their directions, these major faults can be grouped as follows.

NE–SW major faults essentially dominate the Alpine domain. The Zaghouane fault shows an overlapping to the southeast. This fault was primarily active in the Jurrassic. The Tunis–Elles fault continued to Bakaria in Algeria, with a length of 250 km (Jauzein 1967). This fault presents gaps, thinning, and local overlapping caused by reverse faults. The Teboursouk fault extends by the Triassic salt structures at Lansarine, Fej Lahdhoum, Kebouche, and is characterized by the overlapping of the Tebousouk. The Guardimaou–Cap Serat fault separates the Algerian and Tunisian blocs and is marked by volcanic rock manifestations and diapirism.

NW–SE major faults appear in the southern part of Tunisia. They include the Jefara–Gafsa fault system that separates the Atlas zone from the Saharan platform. This system contains the Gafsa and Mednine faults. The Mio-Pliocene basin border faults also follow the NW–SE direction (Fig. 2).

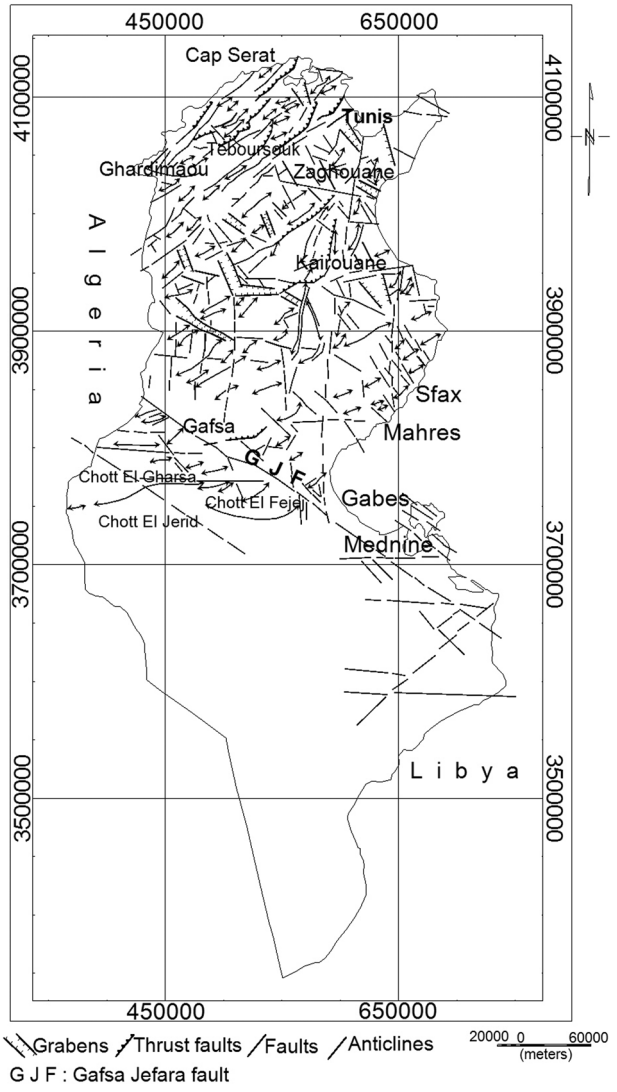

Figure 2 Tectonic Tunisia map adapted from Bouaziz et al. (2002) and Tunisia geological map.

TUNISIAN GRAVITY MAP

Between 1948 and 1967, oil companies conducted many surveys over their permits, e.g., SEREPT, i.e., Sahel (1948), Cap Bon (1950) and Kairouane (1967) permits; AGIP, i.e., Sud and Bir Aouine permits (1951); and Mobil, i.e., Gafsa and Gabès permits (1951). There are many more. To establish the regional Tunisian gravity map from these data, Petroleum Activity Tunisia Enterprise (ETAP, 1982), completed a gravity survey in the extreme north and compiled all the data to establish the gravity map with approximately one station per 25 km^2.

The compilation operation was used to homogenize all the data. Field gravity data were corrected for Earth tides and instrumental drift and converted to absolute gravity values. The international gravity Formula of 1967 is used to reduce the field data. Then, the usual free air, Bouguer, and terrain corrections were applied; the reduction density used was 2.67 g/cm^3.

The Tunisian gravity map used in this paper was established using a grid generated from the digitized points of the Bouguer anomaly map presented by ETAP (1982). This grid is accepted after a cross-validation of data based on a statistical analysis of the differences between digitized Bouguer anomaly and calculated grid values, which gives an average of the differences of 0.01 mGal and a standard deviation of 1.06 mGal. The values of the Bouguer anomaly vary between −85 mGal in the western part of central Tunisia and 40 mGal in the northern part of Tunisia. They are generally comparable with those of the map established in 1982 (−86 mGal

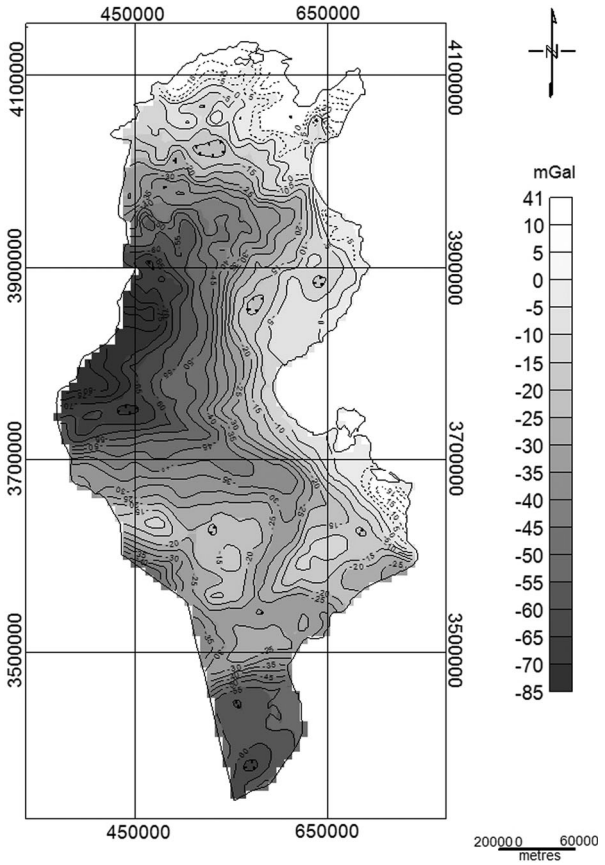

Figure 3 Bouguer anomaly map of Tunisia.

and 47 mGal). The Bouguer anomaly map adopted from this study is dominated by:

- long-wavelength negative anomalies in the Tunisian Atlas, the Chotts Zone, and the Oriental Erg Basin;
- long-wavelength positive anomalies associated with the Tell, the Sahel, and the southeastern coastal zones. Other positive anomalies of maximum amplitude of -10 mGal occupy the Algerian anticlinorium (Fig. 3).

High gradients of the Bouguer anomaly are associated with significant structural alignment. It is clearly observed in the level of the N–S axis, the South of the Chott El Jerid, and between the Algerian anticlinorium and the Oriental Erg Basin. The most outstanding high-gradient zone is the Kairouane–Ghardimaou NW–SE alignment, which appears affected in the north by other alignments. This high gradient constitutes the gravity effect of a major fault that can be expected to affect the upper and lower crusts. We discuss this alignment in more details later.

The regional aspect of the Tunisian Bouguer anomaly map is characterized by long wavelengths that reflect only the gravity effects of the thick sedimentary units, combined with major faults and density contrast effects inside the lithosphere. Thus, the Bouguer anomaly map is largely correlated with the major structural province map of Tunisia (Jallouli and Mickus 2000). The gravity anomalies of the Tell and the Tunisian Atlas are mainly due to variations in the thickness and density of the sedimentary sequences.

The positive anomaly associated with the Sahel is limited to the West by the high gradient defining the North–South axis. This axis is observed throughout the Sahel. It is not simply a response to a change in density of Mio-Plio-Quaternary outcrops dominating this region. It is due probably to the rising of the basement towards the east and to a thinning of the crust.

The Oriental Erg Basin presents an anomaly of −60 mGal crossing the image of the Tunisian part of the Illizi Basin, which extends from the Southeast of Algeria in the West through to Libya in the east (Jallouli and Mickus 2000). The Algerian Anticlinorium is represented by a relatively positive anomaly of −10 mGal.

According to the above discussion, we identify five anomalous zones on the Bouguer anomaly map where boundaries are indicated by at least one high gradient zone. These zones are: the Tell, the Tunisian Atlas, the Sahel, the Algerian Anticlinorium, and the Oriental Erg Basin.

To better identify the major outcrop structures, a Gaussian regional/residual filter with a standard deviation of 0.007 km^{-1}, is applied in the wavenumber domain to the Bouguer anomaly to determine the residual anomaly associated with relatively shallow sources.

The Gaussian regional/residual filter is a low-pass filter and a high-pass filter characterized by a smoother cutoff process. Residual and regional results from Gaussian filtering are similar to high-pass and low-pass filters, respectively, in that they attenuate low- and high-wavenumber components. Mathematically, a Gaussian regional filter anomaly is obtained by convolution of the Bouguer anomaly with a Gaussian function in the space domain. The regional and residual Gaussian filters are implemented in the wavenumber domain and are given, respectively, in the following:

$$\text{Regional filter}: L(k) = \mathrm{e}^{\left(\frac{k^2}{2k_0^2}\right)}, \tag{1}$$

$$\text{Residual filter}: L(k) = 1 - \mathrm{e}^{-\left(\frac{k^2}{2k_0^2}\right)} \tag{2}$$

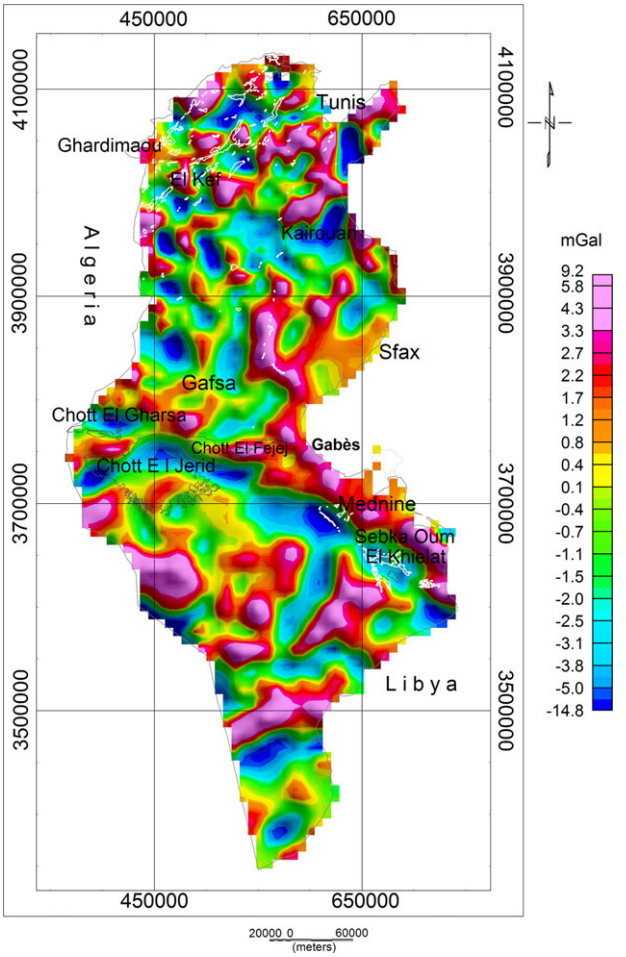

Figure 4 Residual anomaly map after Gaussian filtering. A white line indicates the Triassic outcrops boundary.

where $L(k)$ is the Gaussian filter operator in spectral domain, k is the wavenumber in cycles km^{-1}, and k_0 is the standard deviation of the Gaussian function in km^{-1}.

The Gaussian residual anomaly appears to be the most useful to explain Tunisian geological outcrops. The residual and geological maps present significant similarities.

The residual anomaly shows short-wavelength anomalies that show values ranging from −15 mGal to 9 mGal, with the presence of strong gradients (Fig. 4). This map reveals certain dominant anomaly directions associated with the principal structural zones: the NE–SW direction characterizes northern Tunisia and the Sahel; the NW–SE tendency dominates the north part of the Atlas and the Saharan flexure; the E–W direction characterizes the Oriental Erg and the Chotts zone.

Thus, the structural zones of Tunisia are clearly identifiable on the residual anomaly map (Fig. 4). The extreme northern zone is occupied by NE–SW anomalies having generally positive amplitudes. They are limited towards the south by an E–W band of negative anomalies, which also constitute the northern limit of a succession of negative and positive NE–SW anomalies, translating the effects of the structures of the Tunisian furrow. The spatial shift of these anomalies following the NE–SW direction is probably due to density discontinuities, which particularly affect the NW–SE and N–S directions. The majority of the Triassic outcrops of Northern Tunisia are in relation to the anomaly boundaries occupied by NE–SW discontinuities (Fig. 4).

The NW–SE negative anomalies of the northern part of the Atlas coincide with Mio-Plio-Quaternary basin fillings; they are separated by excess mass anomalies associated with uplift structures. The Sahel, dominated by Mio-Pliocene and Quaternary outcrops (Fig. 1b), is represented by deficits and excesses in mass anomalies that are oriented NE–SW and, respectively, associated with collapse and uplift structures affected by faults. The Sfax area is occupied by a relatively broad anomaly of 1 mGal. In the west, an N–S anomaly with a maximum amplitude of 9 mGal is associated with the N–S axis structures. This feature disappears towards the north in the level Kairouan area; it appears to be stopped by a NW–SE negative anomaly in relation to the zone of a high Bouguer anomaly gradient described previously (Figs 3 and 4).

The Chotts zone is represented by E–W anomalies, generally uncorrelated with the salt nature of the outcrops. Thus, except for the Chott El Gharsa, which is superimposable with an E–W negative anomaly of minimum of −6 mGal, Chott El Jerid and Chott El Fejej are related partially or completely to positive anomalies.

The northern part of the Chott El Jerid is superimposable on three negative anomalies organized on a flattened arc shape, which is continuous with the southern part of Chott El Fejej. These anomalies could be explained as basins separated by faults, which is an interpretation that is in agreement with the asymmetrical syncline under the Chott (Western Petroleum Corporation 1967; Guederi 1980). The southern part of Chott El Jerid is superimposed on a positive anomaly indicating a depth structure signal different to that observed in the northern part. Chott El Fejej is associated with a positive anomaly reaching a maximum of 5 mGal according to an eroded anticline substratum of the Chott (Western Petroleum Corporation 1967; Guederi 1980).

Starting from Gabès, the coast of southern Tunisia shows a broad positive residual anomaly uncorrelated with outcropping Quaternary deposits. It confirms the presence of the dense structures associated with the Medenine fault. The anomalous

arc of a deficit of mass on the level of the northern part of the Chott El Jerid, as previously discussed, continues towards the SE simultaneously with this anomaly. The Triassic outcrop in this zone is superimposed on a negative anomaly, and it appears to be continuous in depth under the Sebkha of Oum El Khielat.

The Oriental Erg is presented by two negative residual anomalies: an E–W anomaly in the North and an oval form anomaly in the South; they are the gravity response to two sedimentary basins separated by an uplift zone.

TUNISIAN CRUSTAL STRUCTURE

Isostatic anomalies

The comparison between Tunisia Bouguer anomaly map and the topographic one shows that long-wavelength Bouguer anomalies correlate inversely with long-wavelength topography: A significant negative anomaly covers the Tunisian Atlas mountains and a positive anomalous band along the coastal zones of subdued topography. This supports the notion of isostatic compensation. The gravity effect of the relief is compensated at depth by a deficit of mass reflecting a thick crust with a density that is relatively low compared with mantle density. The effects of the mass deficits at the base of the crust generally mask the gravity signal associated with shallower crustal sources.

The regional isostatic anomaly map of Tunisia is established using the local compensation Airy model based on topography, with a density of the land of 2.67 g/cm^3, a contrast of density through the Moho of 0.35 g/cm^3, and a thickness of the normal crust of 30 km. This value is averaged from previous crust studies and the Moho map below determined from gravity data (Fig. 6). The regional isostatic map generally presents long-wavelength anomalies associated with density contrasts between the mantle and the lower crust (Fig. 5a). It shows a broad anomaly of mass deficit on the Tunisian Atlas reaching −74 mGal, closed in the east at an alignment coinciding with the N–S axis and continuous in the West (Saharian Atlas in Algeria). This isostatic anomaly is the response to the significant change of crustal thickness in this zone. Another N–S negative anomaly is observed in the south with relatively low amplitude (−40 mGal). The remainder of the country is covered by a positive regional isostatic anomaly.

The residual isostatic anomaly was calculated by eliminating the gravity effects of large wavelength caused by the isostatic variations associated generally with the lower crust sources.

Table 1 Difference range between Moho depths determined from the three formulas.

Formulas	Difference range
Woollard 1959 – Demenitskaya 1958	0.84 – 7.33
Woollard and Strange 1962 – Woollard 1959	0 –3.35
Woollard and Strange 1962 – Demenitskaya 1958	2.19–3.98

The long wavelength of some isostatic residual anomalies explains the gravity effects of the upper crust (Fig. 5b). Thus, the Atlas trend (NE–SW) appears in the north zone. The Sahel, north zone, and the Algerian Anticlinorium are occupied by positive anomalies, whereas the Chotts Zone and the Oriental Erg are associated with negative anomalies, which reveal the low density nature of the sedimentary sequences (Fig. 5b).

Moho morphology

The Bouguer anomaly usually contains the effect of all lithospheric density variations. It is therefore normal to seek the effects of crustal structure and major deep faults in the gravity data. In this paper, crustal structure relating essentially to the depth and morphology of the Moho discontinuity is approached by the empirical relationship, which is deduced by comparing the gravity anomaly and seismically determined crustal thickness proposed by Woollard (1959) and used by Liu and Yen (1975), Ram Babu (1997), Rivero, Pinto, and Casas (2002), Demenitskaya (1967), Arslan, Akýn, and Alaca (2010), and many others.

The formula proposed by Woollard (1959) is one among various empirical formulas that are generated from the correlation between gravity and Moho depth deduced from seismic observations in distinct regions.

We determine the Moho depth using two formulas proposed by Demenitskaya (1958) and Woollard and Strange (1962). We compare these results with those obtained using the proposed formula below (Woollard 1959) (Table 1).

The Moho depth calculated by the Woollard formula is the closest to the Moho seismic depth following the N–S refraction/reflection profile, from the Geotraverse European project (Buness *et al.* 1992), and we have therefore chosen to use this model for further work.

The Moho discontinuity depth is estimated by the following empirical Woollard (1959) formula (3) deduced experimentally from the linear relation between seismic

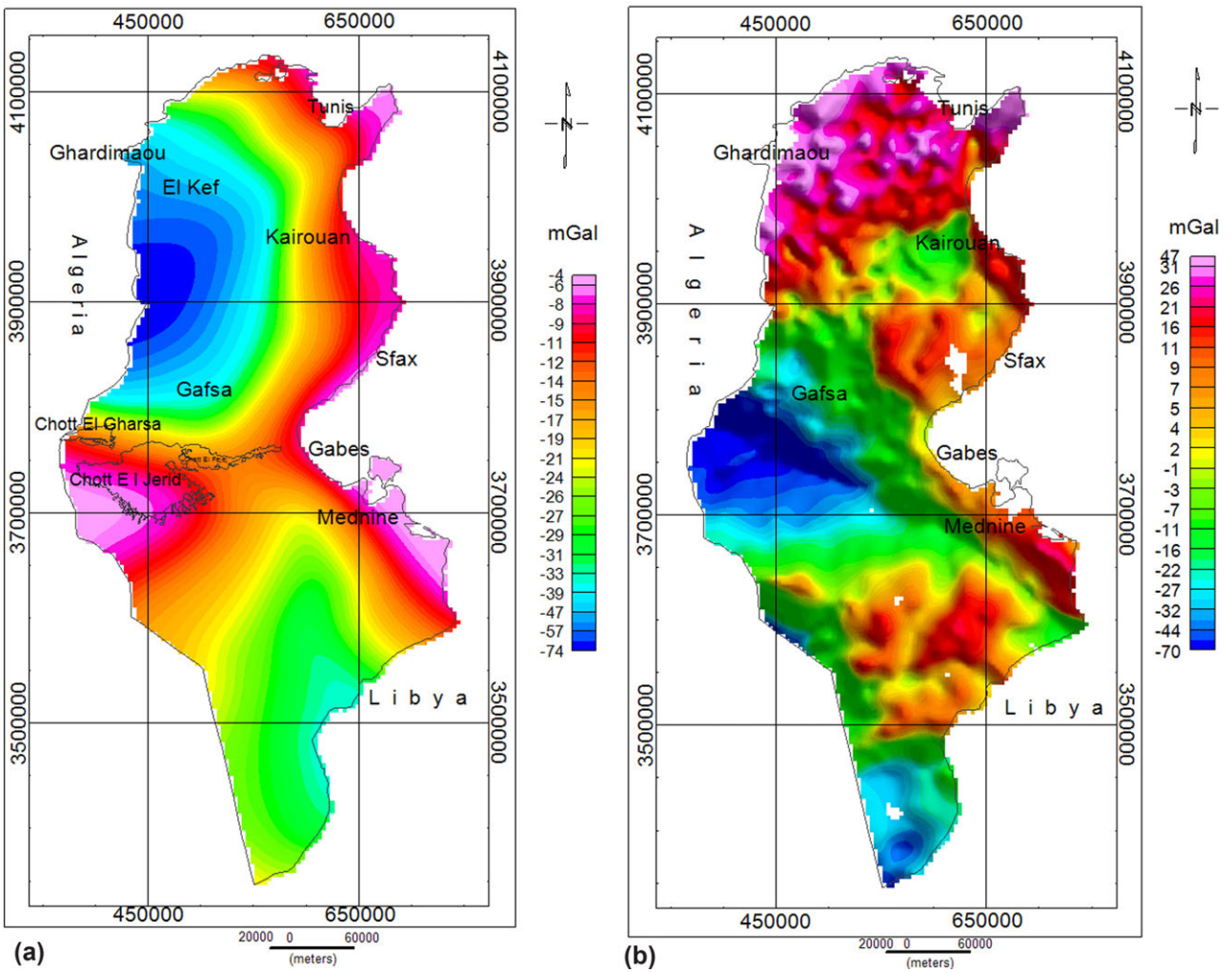

Figure 5 (**a**) Regional isostatic anomaly map, (**b**) Residual isostatic anomaly map.

measurement depth to the Moho discontinuity and Bouguer anomaly proved in various parts of the world.

$$Hm = 32 - 0.08g, \tag{3}$$

where Hm is the Moho depth in km, and g is the regional gravity anomaly in mGal.

The depth of Moho varies between 29 km and 39 km. The crust has a maximum thickness in the Tunisian Atlas region, where the Moho discontinuity deepens gradually towards the West to reach 39 km. This thickening of the crust continues in Algeria (Saharian Atlas). The Moho depth map also shows a relative thinning of the crust in the North of Tunisia (29 km) and in the Sahel (31 km) (Fig. 6).

The comparison of the Moho depth estimated by the present study with the Moho depth estimated by Buness *et al.* (1992) and Mickus and Jallouli (1999), according to an N–S profile, shows a similarity between values with a differences of 2 km in the South and the Atlas and approximately 5 km in the North. On the other hand, the values of the Moho depth presented are roughly comparable with those of the Moho depth map of Europe based on seismic measurements (Molinari and Morelli 2011), which show a variation of Moho depth between 30 km and 40 km beneath Tunisia.

The Moho map shows a typical morphology characterized by a depression in the Tunisian Atlas and in the south. Elsewhere, the surfaces present an uplift zone (Fig. 6). The passage between the depression and uplift zones is marked by a flexure of the Moho surface that coincides in the east and the south with known faults, namely the N–S axis fault and the Gafsa fault. The north flexure must mark an unknown fault, which we name the Kairouan–Ghardimaou fault (Fig. 6).

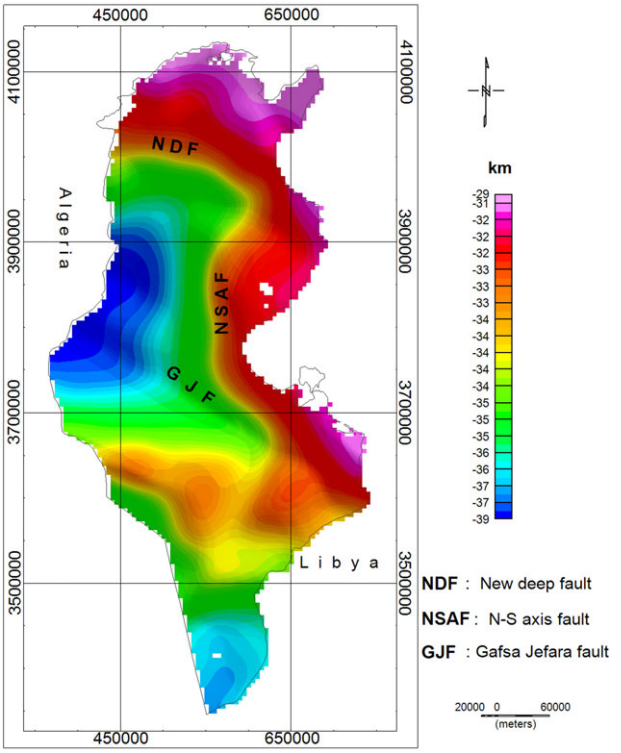

Figure 6 Depth of the Moho discontinuity. NDF: new deep fault, NSAF: North South axis fault, GJF: Gafsa Jeffara fault. The Gafsa and Mednine faults constitute the Gafsa -Jefara fault.

SUPERFICIAL AND DEEP DENSITY DISCONTINUITIES

The horizontal gradient map computed from the Gaussian residual grid shows high gradient features, which constitute zones of density discontinuity (Fig. 7). The Blakely method uses the horizontal gradient peaks to delineate abrupt lateral density changes. They are generally interpreted as faults or contacts (Blakely and Simpson 1986). Taking into account the inhomogeneity of the measurement distribution and the gravity map scale, horizontal gradient peaks revealed by the Blakely method are likely to be responses to major deep faults associated with a significant density contrast.

Thus, the major known normal fault systems of Tunisia should be and are detectable on the horizontal gradient peak map: the Mednine fault with an NW–SE direction appears parallel to the southern coast and continues beyond the Tunisian–Libyan border. The absence of the alignment corresponding to the Gafsa fault is due to the poor gravity data cover of this zone. The Chotts zone is characterized by E–W, NW–SE, and N–S alignments related the faults affecting geologic structures at depth (Fig. 7).

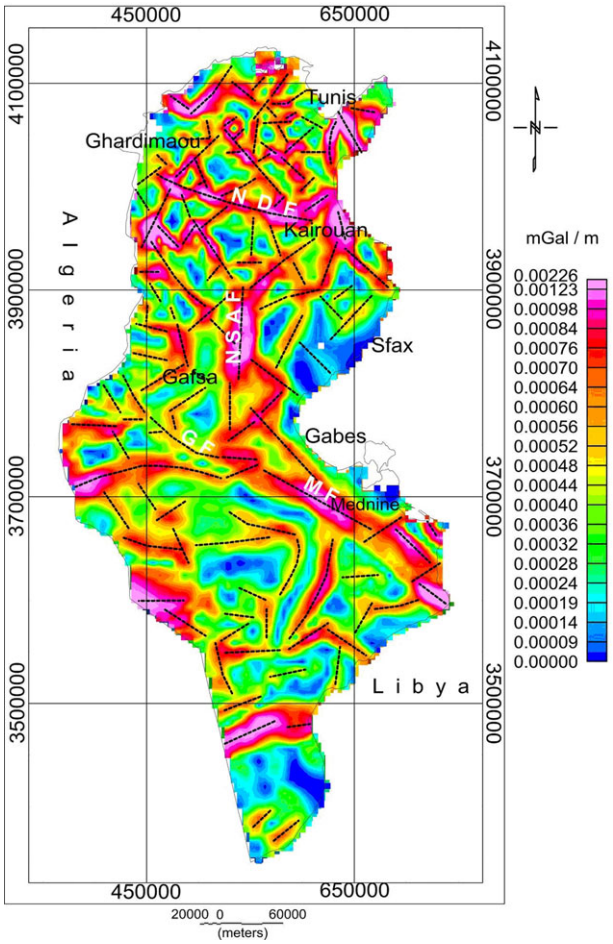

Figure 7 Horizontal gradient map. The black lineaments correspond to faults and discontinuities of density. NDF: new deep fault, NSAF: North-South axis fault, GF: Gafsa fault, MF: Mednine fault. The Gafsa and Mednine faults constitute the Gafsa Jefara fault.

The southern part of the Tunisian Atlas is dominated by E–W, N–S, and NE–SW faults, whereas the northern part of this area is marked by NW–SE discontinuities coinciding with basin border faults. These NW–SE faults, cut by the NE–SW faults in the NW of the Meknassi area, appear in relation to the discontinuities of the same direction and alignment in the Sfax–Mahres area. To the north of the latter area, NE–SW and NW–SE discontinuities affect the non-outcropping Cretaceous. An N–S discontinuity extends in the West of the Sahel; it corresponds to the N–S axis and constitutes a structural limit at which the NE–SW and NW–SE faults of the Atlas and the Sahel terminate (Fig. 7).

The N–S discontinuity disappears in the Kairouan plain area, and the previously described NW–SE discontinuity from Kairouan to Ghardimaou takes its place. It represents a

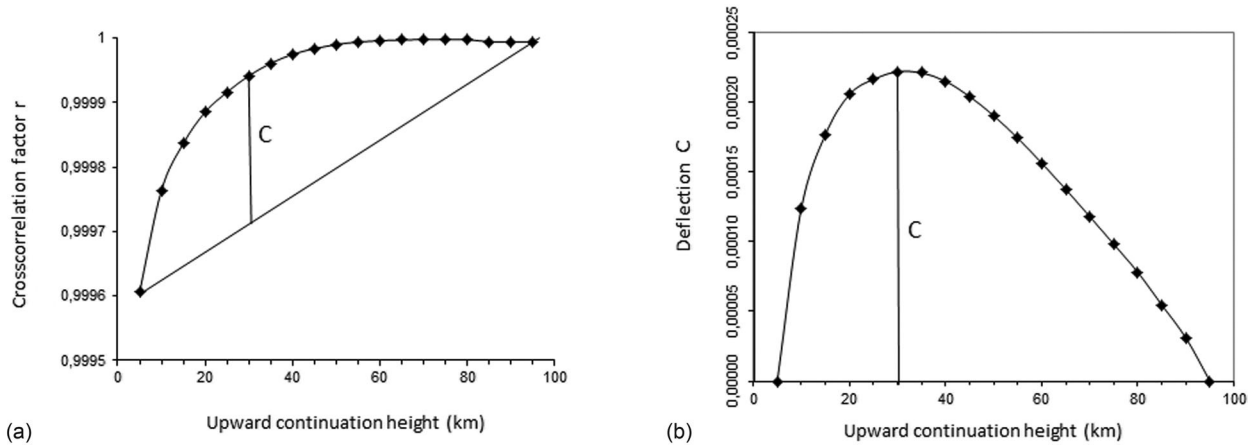

Figure 8 (**a**) Cross-correlations between continuations to two successive heights versus the height, (**b**) Deflection (c) versus the upward continuation height.

regional deep fault. This lineament coincides with the high-gravity-gradient zone in the north of El Kef, which has constituted a paleogeographic boundary during Barremian time (Chikhaoui 2002; Arfaoui *et al.* 2011). This non-outcropping fault is not described by the geologists; it affects deep structures and crust (Fig. 7).

Tunisia presents a tectonic regime typically characterized by NW–SE and NE–SW faults. The majority of the Triassic outcrops are associated with NE–SW discontinuities (Triassic alignments of Dabadib, Tibar, and Lansarin, among others).

To determine deep faults or crustal faults, we determine the horizontal gradient peaks of the upward continuation of the Bouguer anomaly at an optimum height estimate by the method of Zeng, Xu, and Tan (2007). This method is based on the cross-correlation factor r between Bouguer anomaly upward continuations to two successive heights. The cross-correlation factor between two Bouguer anomaly continuations g_1 and g_2 is evaluated by the formula (4) given by Abdelrahman *et al.* (1989):

$$r(g_1, g_2) = \frac{\sum_i^M \sum_j^N g_1(x_i, y_j) g_2(x_i, y_j)}{\sqrt{\sum_i^M \sum_j^N g_1^2(x_i, y_j) \sum_i^M \sum_j^N g_2^2(x_i, y_j)}}, \qquad (4)$$

where M and N are the number of columns and rows of Bouguer anomaly grids, respectively.

The cross-correlation is plotted as a function of the upward continuation height (Fig. 8a). The deflection defined by the difference between the cross-correlation curve and the chord joining its two end points is plotted equally as function of the height. Optimal upward continuation height corresponds to maximum deflection is deduced directly from the deflection curve (Fig. 8b).

In our case, the upward continuation is calculated for heights varying from 5 km to 95 km with a step of 5 km. The optimum upward continuation height estimated by the method of Zeng *et al.* (2007) was 30 km (Fig. 8b).

The different regional anomalies inferred from lesser and greater heights, compared with the optimal one, are dominated by the gravity effects of near-surface sources and deep-seated geological bodies, respectively (Zeng *et al.* 2007).

The NW–SE Kairouane–Ghardimaou, N–S axis, and the Mednine faults persist and constitute the deep structural pattern of Tunisia. The Kairouane–Ghardimaou fault, revealed in this study, continues into Algeria to the west and into the Mediterranean Sea to the east. The three faults constitute a significant limit in the Moho depth map that separates a thin crust zone in the east and north from a thick crust zone in the west, from which it can be deduced that this limit constitutes a Moho flexure origin of these major faults (Fig. 9). The Mednine fault and associated E–W faults affect the Palaeozoic basement (Ben Ayed 1986). The two deepest NW–SE faults are equally associated with the Sirte Basin opening.

In order to determine the crustal deformation caused by the current collision in the Alpine–Himalaya orogeny, Sokoutis *et al.* (2000) built an experimental rheological model composed of three layers: upper crust with a change in the thickness, lower crust, and asthenosphere mantle. Then, they submitted the model to a shortening force. Thus, four major belt systems appeared at different stages of the shortening experiment. The new deep fault (Kairouane–Gardimaou) corresponds to the strike-slip fault affecting the N–S axis in the tectonic Tunisia map presented by Sokoutis et *al.* (2000) that caused the deviation of the N–S axis direction to the east of the part sited north of Kairouan.

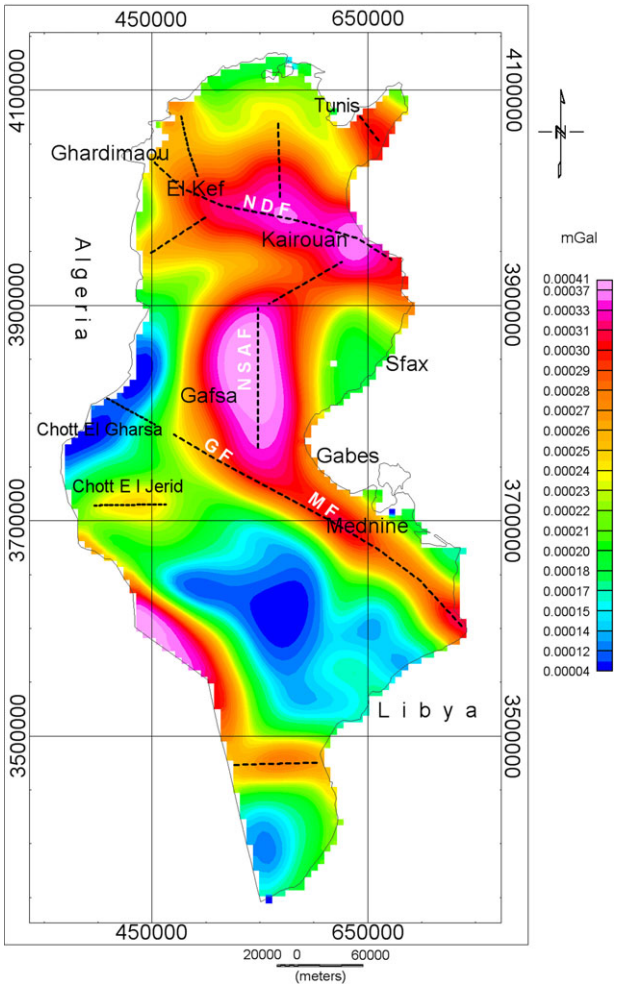

Figure 9 Horizontal gradient after optimal upward continuation of the Bouguer anomaly (30 km). **The black dashed lines indicate deep faults.**

The superficial effects of the NW–SE deep fault are marked by the E–W collapsed structures of the Gaafour–El Aroussa graben and the Mejarda basin bordered by normal faults and marked at their southern borders by structures with no detected anticlinal ending (Figs. 1a and 2).

The tectonic sketch of Tunisia and the Pelagian Sea presented by Burollet (1991) shows an offshore of Eastern Tunisia dominated by NW–SE strike-slip faults and grabens oriented in the same direction as the new deep fault. Burollet (1991) revealed that the NW–SE strike-slip faults and grabens resulted from basement extension associated with shear faults. This suggests and confirms the presence of the new deep fault.

The new NW–SE fault with the N–S axis and the Mednine faults constitute an old conspicuous crustal limit of the Northern and Eastern Tunisia margins, which resulted from early Mesozoic extensional events. They represent equally the west border faults or the intra-continental crust faults of the Mesozoic rift whose centre is apparently in an offshore thinner crust zone (Molinari and Morelli 2011).

Thus, Mesozoic rifting in the Sahel platform and in the north is confirmed by volcanic rocks found in the Triassic, Jurassic, and Cretaceous series in oil wells and outcrops (Ouazaa 2000). In these active crust-thinning stages, N–S and NW–SE rifting control faulting occurs, respectively, in the Sahel platform and in Northern Tunisia. An active post rift subsidence is recognized during the Mesozoic north of the new Kairouane–Ghardimaou deep fault in the Tunisian Furrow where more then 5000 m of Cretaceous series are accumulated (north of El Kef) (Burollet 1956; Jauzein 1967; Chikhaoui 2002). Post-rift subsidence is recognized mainly during Cenozoic time in the Eastern platform (Burollet and Byramjee 1974).

CONCLUSIONS

The major deep faults known in Tunisia as the Mednine and Gafsa faults are recognized by the horizontal gradient peaks, with a new deep fault oriented NW–SE, which runs between Kairouan and Ghardimaou. Crustal structure extended to the entire Tunisian territory based on the morphology of the Moho discontinuity shows conspicuous flexure zones in the surfaces of the latter, which coincide with the deepest faults: NW–SE Kairouan–Ghardimaou, N–S axis, and the Mednine faults. Thus, the new NW–SE Kairouan–Ghardimaou fault revealed by this study is a deep crust fault; it is an important geological significance with critical mineral and oil exploration implications.

ACKNOWLEDGEMENTS

We would like to thank the Editor Prof. Maurizio Fedi, and the Associate Editor and anonymous reviewers for their numerous constrictive suggestions that improved the final version of this manuscript substantially.

REFERENCES

Abdelrahman E.M., Bayoumi A.I., Abdelhady Y.E., Gobashy M.M. and El-Araby H.M. 1989. Gravity interpretation using correlation factors between successive least-squares residual anomalies. *Geophysics* **54**, 1614–1621.

Arfaoui M., Inoubli M.H., Tlig S. and Alouani R. 2011. Gravity analysis of salt structures. An example from the El Kef-Ouargha region (northern Tunisia). *Geophysical Prospecting* **59**, 576–591.

Arslan S., Akýn U. and Alaca A. 2010. Investigation of crustal structure of Turkey by means of gravity data. *Bulletin of the Mineral Research and Exploration* **140**.

Ben Ayed N. 1986. *Evolution tectonique de l'avant-pays de la chaine alpine de Tunisie du début du Mésozoïque à l'actuel*. PhD thesis, Université de Paris Sud, Centre d'Orsay.

Ben Ferjani A., Burrolet P. and Mejri F. 1990. Petroleum geology of Tunisia. *Proceedings of the 3rd Tunisian Petroleum Exploration Conference*, Tunisia, pp. 194.

Bishop W.F. 1975. Geology of Tunisia and adjacent parts of Algeria and Libya. *American Association Geologists Bulletin* **59**, 1033–1058.

Blakely R.J. and Simpson R.W. 1986. Approximating edges of source bodies from magnetic or gravity anomalies. *Geophysics* **51**, 1494–1498.

Bolze J., Burollet P.F. and Castany G. 1952. *Le Sillon Tunisien*, 2nd edn. XIXe Congrès Géologique International.

Bouaziz S., Barrier E., Soussi M., Turki M.M. and Zouari H. 2002. Tectonic evolution of the northern African margin in Tunisia from paleostress data and sedimentary record. *Tectonophysics* **357**, 227–253.

Boukadi N. 1996. Schéma structural nouveau pour le Nord de la Tunisie. *Proceedings of the 5th Tunisian Petroleum Exploration Conference*, Tunisia, Expanded Abstracts, 91.

Buness H., Giese P., Bobier C., Eva C., Merlanti F., Pedone R. *et al*. 1992. The EGT'85 seismic experiment in Tunisia: a reconnaissance of deep structures. *Tectonophysics* **207**, 245–267.

Burollet P.F. 1956. *Contribution à l'étude stratigraphique de la Tunisie centrale*. Annales des Mines et de la Géologie, Tunis.

Burollet P.F. 1991. Structures and tectonics of Tunisia. *Tectonophysics* **195**, 359–369.

Burollet P.F. and Byramjee R. 1974. Evolution géodynamique néogène de la Méditerranée occidentale. *Comptes Rendus de l'Academie des Sciences* **278**, 1321–1324.

Castany G. 1951. L'orogenèse de l'Atlas tunisien. *Bulletin de la Société géologique de France* **6**, 701–720.

Chikhaoui M. 2002. *La zone des diapirs en Tunisie: Cadre structural et évolution géodynamique de la sédimentation méso-cénozoïque et géométrie des corps triasiques*. PhD thesis, Es Sciences Université de Tunis el Manar.

Demenitskaya R.M. 1958. Planetary structures and their reflection in Bouguer anomalies. *Soviet Geology* **8**, 312–319.

Demenitskaya R.M. 1967. *Crust and Mantle of the Earth*. Nedra, Moscow, Russia.

Dubourdieu G. 1956. *Etude géologique de la région de l'Ouenza (confins algéro-tunisiens)*. PhD thesis, Faculté des Sciences d'Alger.

Glangeaud L. 1951. Interprétation tectono-physique des caractères structuraux et paléogéographiques de la Méditerranée occidentale. *Bulletin de la Société géologique de France* **6**, 735–762.

Guederi M. 1980. *Géochimie des sels et des saumures du chott El Jerid (Sud tunisien)*. PhD thesis, Université de Toulouse.

Haller P. 1983. *Structure profonde du Sahel tunisien interprétation géodynamique*. PhD thesis, Fac. SC. et Tech. de l'Université de Franche-Comté.

Jallouli C. and Mickus K. 2000. Regional gravity analysis of the crustal structure of Tunisia. *Journal of African Earth Sciences* **30**, 63–78.

Jauzein A. 1967. *Contribution à l'étude géologique des confins de la dorsale tunisienne (Tunisie septentrionale)*. Annales des Mines et de la Géologie No. 22, Tunis.

Liu C.C. and Yen T.P. 1975. Bouguer anomaly, surface elevation and crustal thickness in Taiwan. *Petroleum geology of Taiwan* **12**, 97–105.

Martinez C. and Truillet R. 1987. Evolution structurale et paléogéographique de la Tunisie. *Mémoire de la Société géologique d'Italie* **38**, 35–45.

Mickus K. and Jallouli C. 1999. Crustal structure beneath the Tell and Atlas mountains (Algeria and Tunisia) through the analysis of gravity data. *Tectonophysics* **314**, 373–385.

Molinari I. and Morelli A. 2011. EPcrust: A reference crustal model for the European plate. *Geophysical Journal International* **185**, 352–364.

Morelli C. and Nicolich R. 1990. A cross section of the lithosphere along the European Geotraverse Southern Segment (from the Alps to Tunisia). *Tectonophysics* **176**, 229–243.

Ouazaa Laaridhi N. L. 2000. *Étude minéralogique et géochimique des épisodes magmatiques mésozoiques et miocènes de la Tunisie*. PhD thesis, Es Sciences Université de Tunis el Manar.

Perthuisot V. 1978. *Dynamique et pétrogenèse des extrusions triasiques en Tunisie septentrionale*. PhD thesis, Ecole Normale Supérieure, Paris.

Perthuisot V. 1981. Diapirism in Northern Tunisia. *Journal of Structural Geology* **3**, 231–235.

Ram Babu H.V. 1997. Average crustal density of the Indian lithosphere: an inference from gravity anomalies and deep seismic soundings. *Journal of Geodynamics* **23**, 1–4.

Rivero L., Pinto V. and Casas A. 2002. Moho depth structure of the eastern part of the Pyrenean belt derived from gravity data. *Journal of Geodynamics* **33**, 315–332.

Rouvier H. 1977. *Géologie de l'extrême-nord tunisien: tectoniques et paléogéographies superposées l'extrémité orientale de la chaîne nord-maghrébine*. PhD thesis, Université Paris VI.

Sokoutis D., Bonini M., Medvedev S., Boccaletti M., Talbot C.J. and Koyi H. 2000. Indentation of a continent with a built-in thickness change: experiment and nature. *Tectonophysics* **320**, 243–270

Snoke A., Schamel S. and Karasek R. 1988. Structural evolution of the Jebel Debadib anticline: A clue to the regional tectonic style of the Tunisian Atlas. *Tectonics* **7**, 497–516.

Turki M.M. 1985. *Polycinématique et contrôle sédimentaire associés sur la cicatrice de Zaghouan-Nebhana*. PhD thesis, Faculté des Sciences de Tunis.

Western Petroleum Corporation 1967. *Chott El Jerid Projet Potasse Tunisien*. Unpublished Report ONM.

Woollard G.P. 1959. Crustal structure from gravity and seismic data measurements. *Journal of Geophysical Research* **64**, 1524–1544.

Woollard G.P. and Strange W.E. 1962. Gravity anomalies and crust of the earth in the Pacific basin. *Geophysical Monograph* **6**, 12.

Zargouni F. 1985. *Tectonique de l'Atlas méridional de Tunisie, évolution géométrique et cinématique des structures en zone de cisaillement*. PhD thesis, Université Louis Pasteur Strasbourg.

Zeng H., Xu D. and Tan H. 2007. A model study for estimating optimum upward- continuation height for gravity separation with application to a Bouguer gravity anomaly over a mineral deposit, Jilin province, northeast China. *Geophysics* **72**, I45–I50.